



**Universiteit
Leiden**
The Netherlands

Quantitative pharmacology approaches to inform treatment strategies against tuberculosis

Mehta, K.

Citation

Mehta, K. (2024, May 30). *Quantitative pharmacology approaches to inform treatment strategies against tuberculosis*. Retrieved from <https://hdl.handle.net/1887/3754903>

Version: Publisher's Version

License: [Licence agreement concerning inclusion of doctoral thesis in the Institutional Repository of the University of Leiden](#)

Downloaded from: <https://hdl.handle.net/1887/3754903>

Note: To cite this publication please use the final published version (if applicable).

Chapter 6

Predictions of bedaquiline central nervous system exposure in tuberculosis meningitis patients using physiologically-based pharmacokinetic modeling

Krina Mehta, Pavel Balazki, Piet H. van der Graaf, Tingjie Guo, J. G. Coen van Hasselt

Clin Pharmacokinet. 2024 Mar 26.

doi: 10.1007/s40262-024-01363-6.

Abstract

Background: The use of bedaquiline as a treatment option for drug-resistant tuberculosis meningitis (TBM) is of interest to address the increased prevalence of resistance to first-line antibiotics. To this end, we describe a whole-body physiologically-based pharmacokinetic (PBPK) model for bedaquiline to predict central nervous system (CNS) exposure.

Methods: A whole-body PBPK model was developed for bedaquiline and its metabolite, M2. The model included compartments for brain and cerebrospinal fluid (CSF). Model predictions were evaluated by comparison to plasma PK time profiles following different dosing regimens and sparse CSF concentrations data from patients. Simulations were then conducted to compare CNS and lung exposures to plasma exposure at clinically relevant dosing schedules.

Results: The model appropriately described the observed plasma and CSF bedaquiline and M2 concentrations from pulmonary TB patients. The model predicted a high impact of tissue binding on target site drug concentrations in CNS. Predicted unbound exposures within brain interstitial exposures were comparable to unbound vascular plasma and unbound lung exposures. However, unbound brain intracellular exposures were predicted to be 7% of unbound vascular plasma and unbound lung intracellular exposures.

Conclusions: The whole-body PBPK model for bedaquiline and M2 predicted unbound concentrations in brain to be significantly lower than the unbound concentrations in the lung at clinically relevant doses. Our findings suggest that bedaquiline may result in relatively inferior efficacy against drug-resistant TBM when compared to efficacy against drug-resistant pulmonary TB.

Introduction

Tuberculosis meningitis (TBM) develops when *Mycobacterium tuberculosis* (Mtb) disseminates from the primary pulmonary site of infection to the central nervous system (CNS) including the brain¹. TBM, the most severe form of Mtb infections, is associated with an approximately 42% mortality rate in hospitalized patient². First-line treatment for drug-susceptible TBM patients remains the same as that for pulmonary tuberculosis patients, which includes a combination of rifampin, isoniazid, pyrazinamide, and ethambutol³. Second-line treatment for TBM patients includes streptomycin, moxifloxacin, fluoroquinolones, cycloserine, linezolid, etc. Several first-line and second-line anti-TB drugs, including, rifampin, ethambutol, and streptomycin, penetrate poorly through the blood-brain barrier (BBB)^{4,43,44}. Second-line drugs, such as, moxifloxacin, fluoroquinolones, ethionamide, cycloserine and linezolid penetrate moderately through BBB⁴. Drug resistant TBM, i.e., Mtb resistant to rifampin and/or isoniazid, is challenging to diagnose and treat. Limited reporting on drug-resistant TBM is attributed to the rarity of the disease and the challenges associated with evaluation of resistance in cerebrospinal fluid (CSF). However, the prevalence of resistance aligns generally with Mtb resistance rates⁵. Currently, there are no standard treatment recommendations for drug-resistant TBM, and treatment approaches are generally selected by treating physicians based on individual patient factors often including extensive treatment with more than five antimicrobial agents. Concerns regarding safety issues of extensive treatments as well as the high mortality rate (69-100%) amongst drug-resistant TBM patients remain a clinical challenge⁶.

Bedaquiline is one of the newer TB antibiotics and was the first novel anti-Mtb drug approved in over 40 years⁷. Bedaquiline has activity against Mtb strains resistant against several first-line and second-line TB therapeutics. Bedaquiline has now been evaluated in over 25 clinical trials as part of various combination regimens against Mtb infections⁸. A combination regimen containing bedaquiline, pretomanid, and linezolid (BPaL) is now recommended for the treatment of rifampin-resistant TB and multidrug-resistant TB patients⁹.

Given the efficacy of BPaL and other bedaquiline-containing combination regimens against drug-resistant pulmonary TB, bedaquiline-containing regimens are being evaluated for the treatment of drug-resistant TBM^{10,11}. Preclinical target site pharmacokinetic (PK) studies reported brain-to-plasma exposure ratio ranging from 2-20%)¹²⁻¹⁴; however, these studies do not differentiate between total and unbound exposures in the brain. In a preclinical efficacy study, combination

therapy with BPaL showed significantly inferior efficacy compared to first-line anti-TB therapy in a mice TBM model following equivalent to human clinically relevant dosing for each drug¹⁴. On the other hand, comparable efficacy was observed following BPaL compared to first-line anti-TB therapy in a mice pulmonary model following equivalent to human clinically relevant dosing for each drug^{15,16}. In pulmonary TB patients, bedaquiline and its active metabolite, M2, concentrations in CSF have been reported to be approximately equivalent to unbound plasma concentrations¹¹. No clinical data on the efficacy of bedaquiline-containing regimens for the treatment of TBM are available^{14,17}. Overall, these contrary preclinical results and very limited clinical data are neither in favor of nor against the suitability of bedaquiline for the treatment of TBM.

Understanding of mechanisms behind the contradicting preclinical results can be useful in future preclinical and clinical study designs. Factors such as molecular weight, lipophilicity, protein binding, ionization, brain metabolism, and transporters play a role in drug distribution across BBB and blood-CSF-barrier (BCSFB), and the extent of unbound drug available to exert the effect. Physiologically-based pharmacokinetic (PBPK) models integrate prior knowledge about physiological processes with the drug's physicochemical and kinetic parameters to enable PK predictions of a drug within various tissue compartments. Thus, PBPK models are well suited to predict bedaquiline concentrations at the target sites-of-action, i.e., CSF, brain interstitial, and intracellular in TBM patients to evaluate its potential for the treatment of MDR TBM patients. However, a whole-body bedaquiline PBPK model with CNS compartments has not yet been developed. In this work, we aimed (1) to develop and evaluate a whole-body PBPK model for bedaquiline and M2 including CSF compartment using plasma and CSF drug and M2 concentrations data from TB patients, (2) to simulate target site concentrations for bedaquiline and M2 for currently recommended bedaquiline dosing schedules in humans.

Methods

Data

Plasma PK data from pulmonary TB patients were accessed through the Platform for Aggregation of Clinical TB Studies (TB-PACTS; <https://c-path.org/programs/tb-pacts/>). We first utilized bedaquiline and M2 physicochemical characteristics and plasma PK data from pulmonary TB patients from a clinical study for the model development. Mean plasma bedaquiline and M2 concentrations by nominal time following bedaquiline doses of 400 mg on Day 1, 300 mg on Day 2, and 200 mg on

Day 3 through 14 (referred to as 400-300-200 QD hereinafter) from a Phase 2 study were used for model fitting¹⁸. Next, the model was validated by comparing typical patient plasma PK predictions with observed data for four different dosing groups, including 200-100 mg QD, 500-400-300 mg QD, and 700-500-400 mg QD dosing in TB patients, from a Phase 1 study, NCT01215110. Lastly, sparse steady-state individual (n=7) plasma and CSF PK data, one sample per patient, for bedaquiline and M2 following bedaquiline 400 mg QD followed by 200 mg three times a week at week 24 were obtained from the literature and were used for further validation of the CNS distribution component of the model¹¹.

Whole-body PBPK model development

The standard PK-Sim whole-body PBPK structural model for small molecules was utilized to build a combined bedaquiline and M2 model¹⁹⁻²¹. The standard PK-Sim whole-body PBPK model consists of key tissues and organs, including, the brain, heart, lungs, liver, kidneys, GI tract, etc., connected through vascular and arterial blood circulation. Each compartment is divided into four sub-compartments, i.e., vascular, blood cells, interstitial, and intracellular²⁰. Physicochemical parameters for bedaquiline and M2 were obtained from the literature (**Table 6.1**)²². Different values have been reported in the literature for bedaquiline lipophilicity and fraction unbound; therefore, model evaluation using each of the reported values was conducted to select the lipophilicity and fraction unbound values that provide the best fit to bedaquiline plasma PK data^{22,23}. Bedaquiline oral absorption has previously been described as atypical with delay and double peaks²⁴⁻²⁶. The Weibull absorption model built within the PK-Sim software was selected due to its flexibility in describing atypical absorption profiles, and the parameters were estimated by fitting to the plasma PK data. Partition coefficients and cellular permeability parameters of bedaquiline and M2 in various tissues were calculated using the PK-Sim standard method^{20,27}. In PK-Sim, the standard calculation method uses lipophilicity and plasma protein binding parameters along with lipid, protein, and water fractions in each compartment and sub-compartment to calculate partition coefficients. CYP3A4 enzyme is involved in the metabolism of bedaquiline to M2²³. Therefore, CYP3A4-mediated metabolism conversion from bedaquiline to M2 was modeled using the Michaelis-Menten equation. Experimental data also suggest contributions of CYP2C8 and CYP2C19 enzymes in the metabolism of bedaquiline to M2 and thus were evaluated in the model using the Michaelis-Menten equation. Expression profiles for all three enzymes based on the RNA-seq method were obtained from the Bgee (<https://www.bgee.org/>) database accessible within PK-Sim²⁸. The parameter Michaelis-Menten constant (Km) for the enzymatic reactions

was obtained from literature from in vitro experiments²⁹. Residual bedaquiline liver plasma clearance and M2 liver plasma clearance estimates were obtained from literature²². Next, the model was simultaneously fitted to bedaquiline and M2 PK data following 400-300-200 QD dosing in pulmonary TB patients to estimate Weibull absorption parameters and enzymatic reaction rates (Vmax) parameters. The combined bedaquiline – M2 plasma PK model was validated by comparing the simulations vs. observed plasma PK data for bedaquiline following 200-100 mg QD, 500-400-300 mg QD, and 700-500-400 mg QD dosing regimens (Clinical Trial: NCT01215110). M2 PK data for this study was not available.

CNS PBPK model development

The standard PK-Sim whole-body PBPK structural model included the following brain sub-compartments: plasma, blood cells, interstitial, and intracellular. Drug permeability across the blood-brain barrier (BBB) is empirically accounted for as half of the transmembrane permeability calculated from physicochemical properties to account for lipid bilayer³⁰. Bedaquiline is not known to be a substrate of transporters located at BBB such as P-gp, BCRP, and MRPs²³. Therefore, the contribution of such transporters in bedaquiline distribution to the brain was not incorporated. The model was then extended in Mobi to incorporate two CSF compartments, cranial- and spinal CSF. The processes of drug distribution to and from CSF were adapted from literature and are illustrated in **Figure 6.1 A**^{31,32}. Flow rates to and from CSF were calculated based on the CSF production rate based on physiological knowledge as discussed in the literature^{31,33} (**Table 6.2**). The same permeability parameter calculated from physicochemical properties was used for diffusion across blood-CSF-barrier (BCSFB) and BBB. The partition coefficient between plasma and CSF was calculated by incorporating fractions of water, lipid, and protein albumin in CSF as shown in equation below and **Table 6.2**^{27,34,35}. To validate the bedaquiline-M2 whole-body PBPK model including CNS components, plasma and brain interstitial compartment predictions for bedaquiline and M2 were compared against the observed data¹¹.

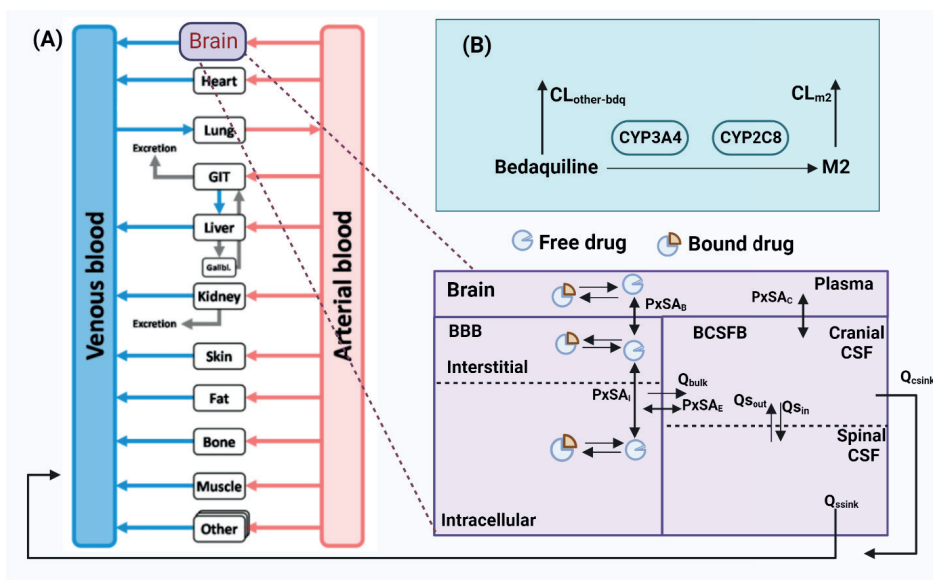
$$PC_{csf} = Fw_{csf} + Alb_{CSF:Plasma} * \frac{1}{fup} - Fw_{plasma} * fup$$

Here, $Alb_{CSF:Plasma}$ = albumin CSF to plasma ratio, fup = fraction unbound in plasma, Fw_{csf} = fraction of water in CSF, Fw_{plasma} = fraction of water in plasma, PC_{csf} = Plasma-to-CSF partition coefficient.

Sensitivity analysis

A local sensitivity analysis was conducted to understand the impact of parameter uncertainty on bedaquiline and M2 plasma and brain intracellular exposure, AUC_{0-t} . Lipophilicity and CNS distribution-related parameters, such as partition coefficients, permeability, and flow rates, were varied 2-fold. Fraction unbound for both bedaquiline and M2 was varied 1000-fold to cover the uncertainty range. Sensitivity analyses were run in Mobi for a typical subject following clinically relevant dosing, 400 mg QD for 14 days followed by 200 mg three times a week, and a sensitivity index was calculated.

Figure 6.1. Illustration of the Bedaquiline-M2 whole-body PBPK model with CNS. The whole-body PBPK model for bedaquiline and M2 was developed in PK-Sim¹⁹⁻²¹. Enzymatic metabolism from bedaquiline to M2 is driven by CYP3A4 and CYP2C8. Additionally, bedaquiline is eliminated at clearance rate $CL_{other-bdq}$ and M2 is eliminated at rate CL_{M2} . There are four routes for unbound drugs to distribute within CSF and brain – (1) from plasma into brain interstitial space, from brain interstitial into brain intracellular, and (2) from plasma into cranial CSF, then into spinal CSF, (3) from cranial CSF to intracellular space, (4) from cranial and spinal CSF into venous blood plasma. Drugs in interstitial and intracellular spaces can bind to the compartment lipid and protein content. The drug goes through mass transfer driven by CSF flow within cranial and spinal sub-compartments of CSF and also to vascular blood. BBB=blood-brain barrier, BCSFB=blood-cerebrospinal fluid barrier, $CL_{other-bdq}$ =additional bedaquiline hepatic clearance (other than M2-relevant clearance), CL_{M2} =M2 clearance, CSF=cerebrospinal fluid, $PxSA_B$ =permeability surface area product for BBB, $PxSA_C$ =permeability surface area product for BCSFB, $PxSA_E$ =permeability surface area product from brain intracellular to cranial CSF, Q_{bulk} =mass transfer flow rate from intracellular to cranial CSF, Q_{csink} =CSF flow rate from cranial CSF to peripheral venous blood, Q_{sin} =CSF flow rate from cranial CSF to spinal CSF, Q_{sout} =CSF flow rate from spinal CSF to cranial CSF, Q_{ssink} =CSF flow rate from spinal CSF to peripheral venous blood. Figure generated using Biorender.com.



Simulations

Simulations were conducted to predict target site, brain intracellular and interstitial, concentrations for bedaquiline and M2 for clinically relevant bedaquiline dosing schedules in a typical TB patient. A typical virtual TB patient was defined as an individual with 60 kg body weight, and 4.32 $\mu\text{mol/L}$ and 2.56 $\mu\text{mol/L}$ as reference concentrations of CYP4A4 and CYP2C8, respectively^{18,28}. Typical virtual patient simulations were conducted for the currently approved dosing regimen and an alternative dosing regimen that was suggested to provide an improved benefit-risk ratio in patients with pulmonary TB³⁶. Thus, the following dosing regimens were simulated: (1) current standard bedaquiline dosing which is 400 mg QD followed by 200 mg three times a week, and (2) alternative 200 mg QD for 8 weeks followed by 100 mg QD. Longitudinal total and unbound bedaquiline and M2 concentrations in peripheral blood plasma, lung intracellular, brain intracellular, and spinal CSF were simulated.

Software

Physiologically-based PK modeling and simulation was performed in PK-Sim® and MOBI® (Open Systems Pharmacology Suite (OSPS), v11.0, www.open-systems-pharmacology.org)³⁷. Statistical analysis and plots were generated in R (R for Windows, v4.1, <https://www.r-project.org/>) using RStudio (RStudio, v1-554, www.rstudio.com/).

Results

The whole-body PBPK model described the observed PK data from plasma and CSF of TB patients.

The final model contained the whole-body PBPK structure with an extended CNS distribution model for both bedaquiline and M2. Multiple literature-based values have been reported in the literature for bedaquiline lipophilicity and fraction unbound, and the values that provided the best fit to observed plasma PK data were retained in the final model (**Table 6.1**)^{22,23}. Enzymatic conversion of bedaquiline to M2 was first set up to be mediated by CYP3A4, CYP2C8, and CYP2C19; however, V_{max} for CYP2C19-mediated reaction was estimated to be very low and thus was not retained²⁹. The CNS component of the model contained the brain compartment that included plasma, interstitial, cranial CSF, spinal CSF, and intracellular sub-compartments. The parameters relevant to CNS distribution were described based on physiological and drug-specific knowledge (**Figure 6.1, Table 6.2**)³⁰⁻³³.

The final bedaquiline-M2 whole-body PBPK model predictions agreed adequately with the observed plasma PK data for both bedaquiline and M2 following bedaquiline 400-300-200 QD dosing (**Figure 6.2A**)¹⁸, as well as four different bedaquiline dosing regimens (**Figure 6.2B**). Additionally, simulated bedaquiline and M2 PK profiles agreed very well with the observed plasma PK data in patients following current clinically recommended bedaquiline dosing (**Figure 6.3**). At Week-24, predicted 24 hr plasma average concentrations (C_{avg}) for bedaquiline and M2 were 718 ng/mL and 268 ng/mL, respectively. These results matched reasonably well with the reported 24-week plasma concentrations for both bedaquiline and M2 in literature following current clinically recommended bedaquiline dosing (median (IQR) concentrations 1264 ng/ml (910-2244) and 252 ng/ml (34-290) for bedaquiline and M2, respectively, based on data from 13 patients)³⁹. At Week-8, predicted peripheral vascular blood cell to plasma concentration ratios were 0.54 and 19.5 for bedaquiline and M2, respectively (**Table 6.3**). These results matched reasonably well with the reported peripheral blood mononuclear cells to plasma concentrations ratio in literature at Week-8 (1.1 and 22.2 for bedaquiline and M2, respectively)⁴⁰.

The model slightly underpredicted mean bedaquiline and M2 concentrations in spinal CSF; however, the CSF concentrations were within a standard deviation of the observed CSF concentrations (**Figure 6.3**). Given that the CNS concentrations were bottom-up predictions based on physiological and drug-specific knowledge and that only sparse CSF observed data points (n=7) are available to date, the model was deemed reliable for the objectives of this study.

Table 6.1. Parameters for the Bedaquiline-M2 PBPK model with CNS distribution.

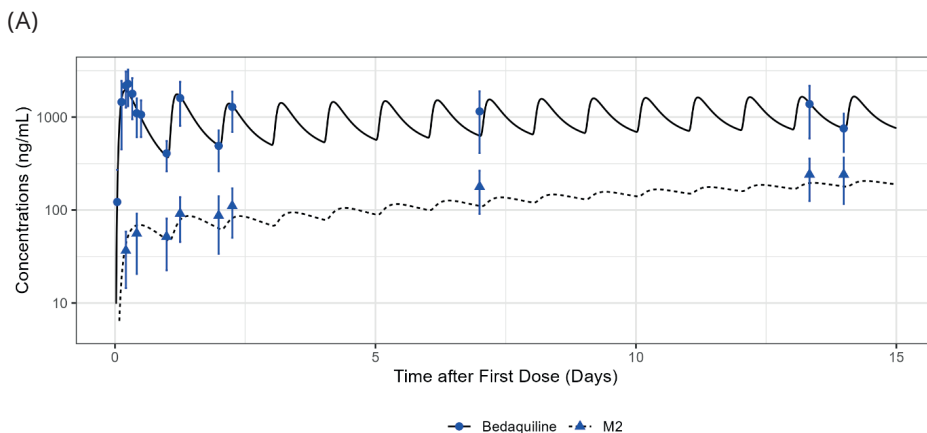
Parameter	Unit	Value	Source
Bedaquiline^a			
Molecular Weight ^b	g/mol	555.5	PubChem Database
Lipophilicity	Log unit	5.14	²²
Fraction unbound in plasma	Dimensionless	0.0003	²²
pKa (Base)	Dimensionless	9.10	²²
Weibull dissolution time (50% dissolved)	Min	125.21	Estimated
Weibull dissolution shape	Dimensionless	1.51	Estimated
V _{max} CYP3A4	umol/L/min	407.85	Estimated
K _m CYP3A4	umol/L	8.5	²⁹
V _{max} CYP2C8	umol/L/min	163.73	Estimated
K _m CYP2C8	umol/L	13.1	²⁹
Additional hepatic clearance	L/hr/kg	0.03	²²
Permeability across BBB and BCSFB (assumed half of the calculated permeability from plasma-to-interstitial due to lipid bilayer in BBB and BCSFB)	dm/min	0.00217	PK-Sim Calculated
Cellular permeability from plasma to interstitial	dm/min	0.013	
Brain Interstitial-water partition coefficient	Dimensionless	0.0013	
Brain Intracellular-water partition coefficient	Dimensionless	6.2E-05	
Plasma-to-CSF partition coefficient	Dimensionless	0.0082	Calculated (see equation 1)
M2			
Molecular Weight ^c	g/mol	541	PubChem Database
Lipophilicity	Log unit	6.5	²²
Fraction unbound in plasma	Dimensionless	0.0005	²²
Hepatic clearance	L/hr/kg	0.14	Estimated
Permeability across BBB and BCSFB (assumed half of the calculated permeability from plasma-to-interstitial due to lipid bilayer in BBB and BCSFB)	dm/min	0.185	PK-Sim Calculated
Cellular permeability from plasma to interstitial	dm/min	0.36	
Brain Interstitial-water partition coefficient	Dimensionless	0.0013	
Brain Intracellular-water partition coefficient	Dimensionless	2.8E-06	
Plasma-to-CSF partition coefficient	Dimensionless	0.0084	Equation 1

Table 6.2. Key physiological parameters for the CNS distribution of the PBPK model.

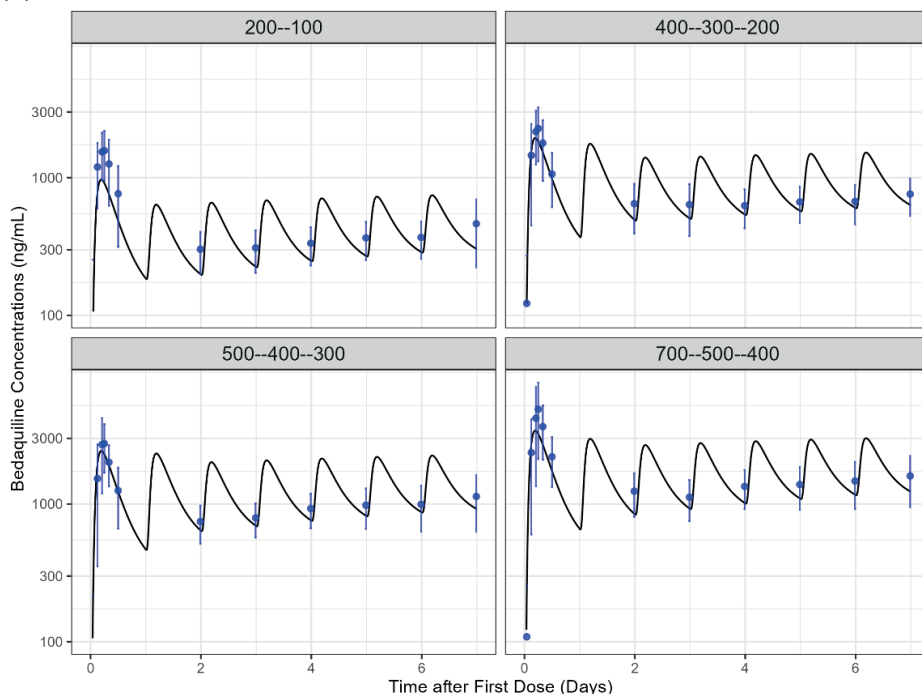
Parameter	Unit	Value	Source
Albumin CSF-plasma ratio	Dimensionless	0.008	35
CSF lipid fraction	Dimensionless	0.0573	
CSF protein fraction	Dimensionless	0.005	
CSF production rate (Qcsf) ^a	mL/min	0.42	32
Surface area of blood-brain-barrier (BBB) (SA _b)	cm ²	150000	
Surface area of blood-CSF-barrier (BCSFB) (SA _c)	cm ²	15000	
Surface area brain interstitial – intracellular (SA _i)	cm ²	3686	41

^a CSF production rate was not directly used as a parameter; however, flow rates across the brain - CSF - peripheral blood were calculated based on CSF production rate as follows based on literature: $Q_{bulk} = 0.25 * Q_{csf}$, $Q_{ssink} = 0.38 * ((0.75 * Q_{csf}) + Q_{bulk})$, $Q_{sout} = 0.9 * Q_{ssink}$, $Q_{sin} = Q_{sout} + Q_{ssink}$, $Q_{csink} = 0.75 * (Q_{csfprod} + Q_{bulk} - Q_{sin} + Q_{sout})$; Permeability surface area product across brain intracellular to cranial CSF ($PxSA_c$) was set to high value, 300, assuming no barrier based on literature^{22,23}

Figure 6.2. Predicted and observed plasma PK profiles for (A) model fitting dataset, and (B) model validation dataset. The final bedaquiline-M2 whole-body PBPK model predictions agreed well with the observed plasma PK data for both bedaquiline and M2 following bedaquiline 400-300-200 QD dosing, and four different bedaquiline dosing regimens from a Phase 1 study. Dosing regimens were administered in increasing amounts for the first three days of the therapy. I.e., 400-300-200 mg QD represents 400 mg on Day 1, 300 mg on Day 2, and 200 mg QD on Day 3 onwards.



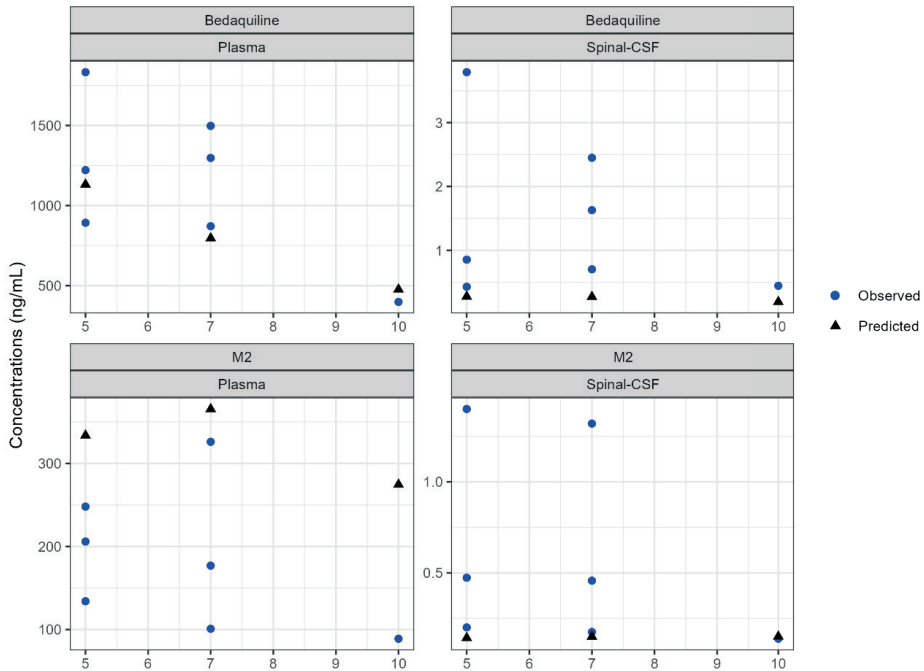
(B)



Local sensitivity analysis elucidates the influence of uncertainty in parameters on drug exposures.

The overall impact of reported uncertainties in key physicochemical parameters, lipophilicity, and plasma protein binding, on vascular plasma and CNS drug exposure (AUC_{0-t}) was evaluated by using local sensitivity analysis. A two-fold decrease in bedaquiline lipophilicity (i.e., 5.12 to 2.5) was predicted to decrease brain intracellular unbound AUC_{0-t} by 65.2% and vascular plasma AUC_{0-t} by 24%. A two-fold increase in albumin CSF-to-plasma ratio (i.e., 0.008 to 0.016) was predicted to increase brain intracellular total and unbound AUC_{0-t} by 0.4%. A 1000-fold increase (i.e., 0.0003 to 0.3) in bedaquiline fraction unbound was predicted to decrease brain intracellular unbound AUC_{0-t} by 55.2% and vascular plasma AUC_{0-t} by 40.6%.

Figure 6.3. Bedaquiline and M2 observed vs. predictions for plasma and spinal CSF compartments at steady-state after 9 weeks of treatment. The model reasonably predicted the observed data. Bedaquiline dosing was 400 mg once daily (QD) for 14 days followed by 200 mg three times a week up to 9 weeks. Steady-state concentrations were measured either 3, 5, or 7 hours after the last 200 mg dose. Blue points represent the observed mean and standard deviation. Black points represent typical patients' predicted value.



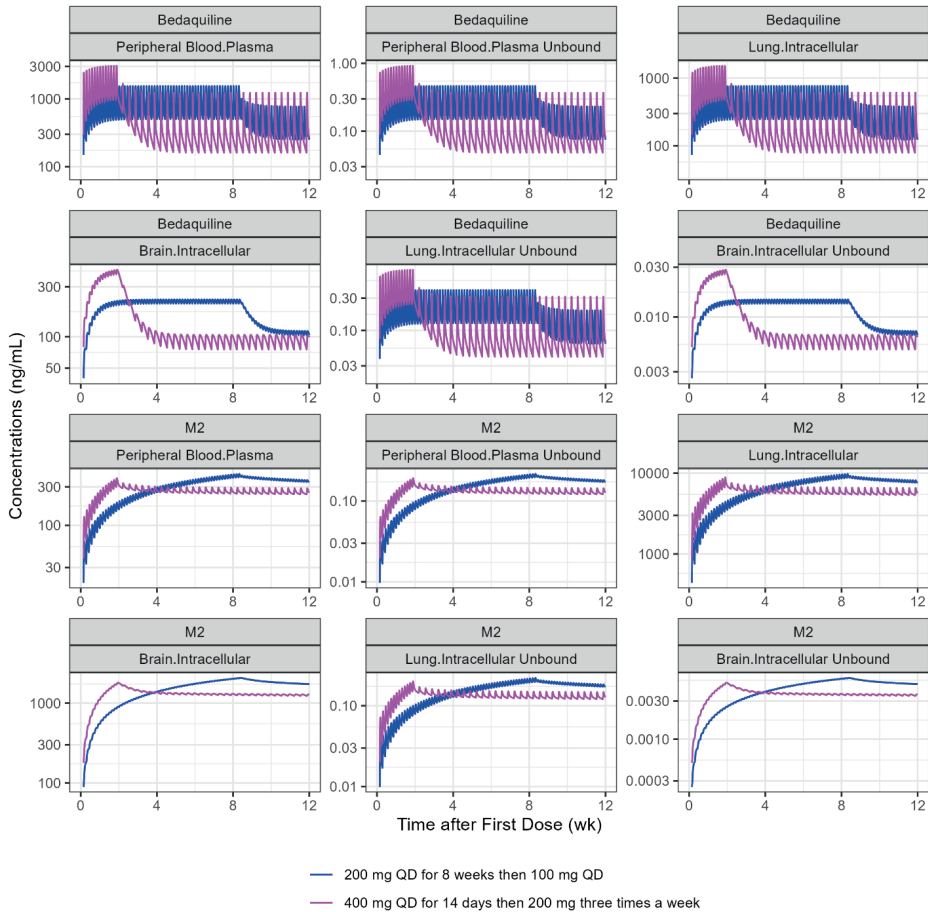
PBPK simulations predicted significantly lower bedaquiline brain concentrations in the intracellular compartment compared to peripheral blood.

Unbound bedaquiline and M2 concentrations in lung interstitial and intracellular, brain interstitial, and CSF were predicted to be comparable to unbound plasma concentrations. However, unbound bedaquiline and M2 concentrations in brain intracellular were predicted to be significantly lower than unbound plasma and unbound lung intracellular concentrations (ratio ~ 0.07 compared to unbound concentrations in plasma) (Figure 6.4, Table 6.3). Additionally, our simulations suggested that 200 mg QD for 8 weeks followed by 100 mg QD would achieve relatively increased plasma concentrations for a longer duration of time when compared to 400 mg QD for 14 days followed by 200 mg three times a week (Figure 6.4).

Table 6.3. Predicted tissue to plasma concentrations ratio for bedaquiline and M2.

Parameter (C_{avg} ratio)	Bedaquiline	M2
Peripheral vascular blood cells / plasma	0.54	19.5
Brain Interstitial / plasma	0.36	0.38
Brain Intracellular / plasma	0.27	4.93
Brain Interstitial Unbound / plasma unbound	0.97	0.99
Brain Intracellular Unbound / plasma unbound	0.07	0.03
Spinal-CSF / plasma unbound	0.97	1.08
Lung Interstitial / plasma	0.38	0.37
Lung Intracellular / plasma	0.49	22.2
Lung Interstitial Unbound / plasma unbound	1.02	1.00
Lung Intracellular Unbound / plasma unbound	0.85	1.00

Figure 6.4. Typical patient simulations of Bedaquiline and M2 concentrations within various CNS compartments following the current and alternative Bedaquiline dosing regimens. The simulations suggested limited availability of unbound bedaquiline and M2 in brain interstitial and intracellular compartments. The model suggested relatively higher concentrations for longer duration for all compartments following the alternative dosing regimen, 200 mg QD for 8 weeks then 100 mg QD, than the current dosing regimen, 400 mg QD for 14 days followed by 200 mg three times a week.



Discussion

We developed a whole-body PBPK model for bedaquiline and M2, coupled with CSF and brain compartments using clinical data. We then used the model to predict bedaquiline and M2 exposures in CNS compartments, including the brain intracellular compartment.

Our PBPK model enabled predictions of bedaquiline and M2 drug concentration-time profiles at target sites-of-action, brain interstitial and intracellular, for TBM

patients. The model predicted a total bedaquiline tissue-to-plasma concentrations ratio of 27% for brain intracellular. This predicted brain intracellular to plasma ratio is relatively comparable to the findings from preclinical studies that reported brain parenchyma to plasma concentrations ratios ranging from 2-20% following oral bedaquiline dosing suggesting the reliability of our model^{12,13}. However, only unbound drug at site-of-action is assumed to be available to exert an anti-bacterial effect. The model-predicted unbound concentrations within brain intracellular compartment were drastically lower as compared to unbound concentrations in plasma and lungs (ratio ~ 0.07 compared to unbound concentrations in plasma) (**Figure 6.4**). We predicted that sub-optimal drug concentrations would be available in brain intracellular to exert effect following bedaquiline at clinically relevant dosing in TBM patients. These predictions may support the experimental findings of inferior efficacy of BPaL combination with that of standard first-line anti-TB therapy in the TBM mouse model following dosing equivalent to human efficacious dosing for each drug¹⁴. Prospective studies comparing the efficacy of various combination regimens with and without bedaquiline in drug-resistant TBM models are suggested. Our model predicted no delay or non-linearity between plasma, brain, and lung tissues (S6.2). This suggests that plasma drug concentrations may be considered as surrogate for tissue concentrations considering relative ratio.

Sensitivity analysis allowed estimation of the impact of known uncertainty in protein binding and lipophilicity parameters on predictions of vascular plasma and CNS concentrations. However, it should be noted that our model was calibrated using observed vascular plasma concentrations and described observed CSF concentrations well. Thus, the estimated parameters of our model would be correlated with protein binding and lipophilicity parameters used in the model development. Therefore, it is unlikely that protein binding and lipophilicity parameters different than those used in our model development would lead to very different predictions of plasma or target site exposures.

We focused on typical TB patient simulations and did not simulate with inter-individual variability (IIV), because direct application of the IIV estimates from PopPK models to the PBPK model often does not appropriately characterize observed variability in plasma PK profiles. Previously, high IIV (>80%) in absorption-related parameters and moderate IIV (~50%) in distribution and clearance-related parameters have been estimated for bedaquiline using empirical population PK models^{24,25}. These IIV estimates translate into moderate IIV in steady-state exposure ($AUC_{ss-weekly}$ interquartile range ~ 90 – 250 ug·hr/mL). Thus, the impact of observed IIV on overall

conclusions would be negligible given the fold difference between predicted total and unbound drug concentrations at the site of action for TBM patients.

Our model described plasma bedaquiline and M2 drug concentration data well for various dosing scenarios. Our typical patient CSF concentration predictions were slightly lower than the observed mean concentrations for both bedaquiline and M2 but were within the observed standard deviation range. Some uncertainty exists in observed CSF concentrations due to the small sample size ($n=7$, one sample for each patient) and bioanalytical challenges due to the high protein binding nature of bedaquiline. The impact of the slight underpredictions of mean CSF concentrations on overall predictions of unbound drug concentrations within the brain intracellular compartment seems negligible given the fold difference between unbound brain intracellular and CSF drug concentrations.

We did not evaluate the impact of TBM disease on bedaquiline and M2 concentrations in CNS. In our model, parameters relevant to drug penetration in CNS were calculated based on physicochemical and physiological parameters, including albumin plasma-to-CSF ratio, obtained from healthy subjects³⁵. Our typical patient CSF concentration predictions were compared against the observed CSF concentrations data from pulmonary TB patients¹¹. Our sensitivity analysis suggested a small impact of albumin plasma-to-CSF ratio on brain concentrations of bedaquiline. However, higher CSF protein levels are associated with increased the partition coefficient for rifampin⁴¹. Future studies should evaluate the impact of TBM disease on bedaquiline PK.

PBPK models including the transporters involved in BBB and BCSFB have been reported in the literature. These models included active transport processes. Key apical efflux transporters involved in blood-brain-barrier or blood-CSF-barrier are P-gp, BCRP, and MRPs³¹. Bedaquiline is not known to be a substrate of any of these transporters²³; therefore, we did not explicitly include brain transporters in this work.

In conclusion, we present a whole-body PBPK model for bedaquiline and its active metabolite coupled with an expanded CNS distribution model, including CSF and brain sub-compartments. The model appropriately described observed plasma and CSF bedaquiline and M2 concentrations from TB patients. However, unbound concentrations in brain intracellular were predicted to be much lower than the predicted unbound concentrations in plasma and lungs. These results can be useful in designing experiments comparing the efficacy of various combination regimens with and without bedaquiline in drug-resistant TBM models.

References

1. Seddon JA, Wilkinson R, van Crevel R, et al. Knowledge gaps and research priorities in tuberculous meningitis. *Wellcome Open Research*. 2019;4:1-18. doi:10.12688/wellcomeopenres.15573.1
2. Navarro-Flores A, Fernandez-Chinguel JE, Pacheco-Barrios N, Soriano-Moreno DR, Pacheco-Barrios K. Global morbidity and mortality of central nervous system tuberculosis: a systematic review and meta-analysis. *J Neurol*. 2022;269(7):3482-3494. doi:10.1007/s00415-022-11052-8
3. Nahid P, Dorman SE, Alipanah N, et al. Executive Summary: Official American Thoracic Society/Centers for Disease Control and Prevention/Infectious Diseases Society of America Clinical Practice Guidelines: Treatment of Drug-Susceptible Tuberculosis. *Clinical Infectious Diseases*. 2016;63(7):853-867. doi:10.1093/cid/ciw566
4. Ramachandran R and Muniyandi M. Towards Improved Treatment Outcomes for Tuberculosis Meningitis - Rethinking the Regimen. *Open access journal of neurology and neurosurgery*. 2018; Volume 8, issue 2. doi: 10.19080/OAJNN.2018.08.555734.
5. Heemskerk AD, Nguyen MTH, Dang HTM, Vinh Nguyen CV, Nguyen LH, Do TDA, Nguyen TTT, Wolbers M, Day J, Le TTP, Nguyen BD, Caws M, Thwaites GE. Clinical Outcomes of Patients With Drug-Resistant Tuberculous Meningitis Treated With an Intensified Antituberculosis Regimen. *Clin Infect Dis*. 2017 Jul 1;65(1):20-28. doi: 10.1093/cid/cix230.
6. Evans EE, Avaliani T, Gujabidze M, et al. Long term outcomes of patients with tuberculous meningitis: The impact of drug resistance. *PLoS One*. 2022;17(6):e0270201. doi:10.1371/journal.pone.0270201
7. Khoshnood S, Goudarzi M, Taki E, et al. Bedaquiline: Current status and future perspectives. *Journal of Global Antimicrobial Resistance*. 2021;25:48-59. doi:10.1016/j.jgar.2021.02.017
8. Andries K, Verhasselt P, Guillemont J, et al. A diarylquinoline drug active on the ATP synthase of *Mycobacterium tuberculosis*. *Science*. 2005;307(5707):223-227. doi:10.1126/science.1106753
9. World Health Organization. Consolidated Operational Guidelines on Handbook Tuberculosis.; 2020.
10. Akkerman OW, Odish OFF, Bolhuis MS, et al. Pharmacokinetics of Bedaquiline in Cerebrospinal Fluid and Serum in Multidrug-Resistant Tuberculous Meningitis. *Clinical Infectious Diseases*. 2015;62(4):523-524. doi:10.1093/cid/civ921
11. Upton CM, Steele CI, Maartens G, Diacon AH, Wiesner L, Dooley KE. Pharmacokinetics of bedaquiline in cerebrospinal fluid (CSF) in patients with pulmonary tuberculosis (TB). *J Antimicrob Chemother*. 2022;77(6):1720-1724. doi:10.1093/jac/dkac067
12. Ordonez AA, Carroll LS, Abhishek S, et al. Radiosynthesis and PET Bioimaging of 76Br-Bedaquiline in a Murine Model of Tuberculosis. *ACS Infectious Diseases*. 2019;5(12):1996-2002. doi:10.1021/acsinfecdis.9b00207
13. Pamreddy A, Baijnath S, Naicker T, et al. Bedaquiline has potential for targeting tuberculosis reservoirs in the central nervous system. *RSC Adv*. 2018;8(22):11902-11907. doi:10.1039/c8ra00984h
14. Mota F, Ruiz-Bedoya CA, Tucker EW, et al. Dynamic 18F-Pretomanid PET imaging in animal models of TB meningitis and human studies. *Nature Communications*. 2022;13(1):7974. doi:10.1038/s41467-022-35730-3
15. Tasneen R, Betoudji F, Tyagi S, et al. Contribution of Oxazolidinones to the Efficacy of Novel Regimens Containing Bedaquiline and Pretomanid in a Mouse Model of Tuberculosis. *Antimicrob Agents Chemother*. 2016;60(1):270-277. doi:10.1128/AAC.01691-15
16. Food and Drug Administration (FDA). FDA Briefing Document Pretomanid Tablet, 200 mg Meeting of the Antimicrobial Drugs Advisory Committee (AMDAC). Published online 2019; <https://www.fda.gov/media/127592/download>.
17. Smith AGC, Gujabidze M, Avaliani T, et al. Clinical outcomes among patients with tuberculous meningitis receiving intensified treatment regimens. *Int J Tuberc Lung Dis*. 2021;25(8):632-639. doi:10.5588/ijtld.21.0159

18. Diacon AH, Dawson R, Von Groote-Bidlingmaier F, et al. Bactericidal activity of pyrazinamide and clofazimine alone and in combinations with pretomanid and bedaquiline. *American Journal of Respiratory and Critical Care Medicine*. 2015;191(8):943-953. doi:10.1164/rccm.201410-1801OC
19. Kuepfer L, Niederalt C, Wendl T, et al. Applied Concepts in PBPK Modeling: How to Build a PBPK/PD Model. *CPT: Pharmacometrics and Systems Pharmacology*. 2016;5(10):516-531. doi:10.1002/psp4.12134
20. Willmann S, Höhn K, Edginton A, et al. Development of a Physiology-Based Whole-Body Population Model for Assessing the Influence of Individual Variability on the Pharmacokinetics of Drugs. *Journal of Pharmacokinetics and Pharmacodynamics*. 2007;34(3):401-431. doi:10.1007/s10928-007-9053-5
21. Willmann S, Schmitt W, Keldenich J, Dressman JB. A Physiologic Model for Simulating Gastrointestinal Flow and Drug Absorption in Rats. *Pharmaceutical Research*. 2003;20(11):1766-1771. doi:10.1023/B:PHAM.0000003373.72652.c0
22. Gaohua L, Wedagedera J, Small BG, et al. Development of a Multicompartment Permeability-Limited Lung PBPK Model and Its Application in Predicting Pulmonary Pharmacokinetics of Antituberculosis Drugs. *CPT: Pharmacometrics and Systems Pharmacology*. 2015;4(10):605-613. doi:10.1002/psp4.12034
23. van Heeswijk RPG, Dannemann B, Hoetelmans RMW. Bedaquiline: A review of human pharmacokinetics and drug-drug interactions. *Journal of Antimicrobial Chemotherapy*. 2014;69(9):2310-2318. doi:10.1093/jac/dku171
24. Svensson EM, Dosne AG, Karlsson MO. Population Pharmacokinetics of Bedaquiline and Metabolite M2 in Patients with Drug-Resistant Tuberculosis: The Effect of Time-Varying Weight and Albumin. *CPT: Pharmacometrics and Systems Pharmacology*. 2016;5(12):682-691. doi:10.1002/psp4.12147
25. McLeay SC, Vis P, Van Heeswijk RPG, Green B. Population pharmacokinetics of bedaquiline (TMC207), a novel antituberculosis drug. *Antimicrobial Agents and Chemotherapy*. 2014;58(9):5315-5324. doi:10.1128/AAC.01418-13
26. Mehta K, Guo T, van der Graaf PH, van Hasselt JGC. Predictions of Bedaquiline and Pretomanid Target Attainment in Lung Lesions of Tuberculosis Patients using Translational Minimal Physiologically Based Pharmacokinetic Modeling. *Clin Pharmacokinet*. 2023;62(3):519-532. doi:10.1007/s40262-023-01217-7
27. Schmitt W. General approach for the calculation of tissue to plasma partition coefficients. *Toxicol In Vitro*. 2008;22(2):457-467. doi:10.1016/j.tiv.2007.09.010
28. Cordes H, Rapp H. Gene expression databases for physiologically based pharmacokinetic modeling of humans and animal species. *CPT: Pharmacometrics & Systems Pharmacology*. 2023;12(3):311-319. doi:10.1002/psp4.12904
29. Liu K, Li F, Lu J, et al. Bedaquiline metabolism: enzymes and novel metabolites. *Drug Metab Dispos*. 2014;42(5):863-866. doi:10.1124/dmd.113.056119
30. Yamamoto Y, Väitalo PA, van den Berg DJ, et al. A Generic Multi-Compartmental CNS Distribution Model Structure for 9 Drugs Allows Prediction of Human Brain Target Site Concentrations. *Pharm Res*. 2017;34(2):333-351. doi:10.1007/s11095-016-2065-3
31. Gaohua L, Neuhooff S, Johnson TN, Rostami-Hodjegan A, Jamei M. Development of a permeability-limited model of the human brain and cerebrospinal fluid (CSF) to integrate known physiological and biological knowledge: Estimating time varying CSF drug concentrations and their variability using in vitro data. *Drug Metabolism and Pharmacokinetics*. 2016;31(3):224-233. doi:10.1016/j.dmpk.2016.03.005
32. Saleh MAA, Loo CF, Elassaiss-Schaap J, De Lange ECM. Lumbar cerebrospinal fluid-to-brain extracellular fluid surrogacy is context-specific: insights from LeicNS-PK3.0 simulations. *J Pharmacokinet Pharmacodyn*. 2021;48(5):725-741. doi:10.1007/s10928-021-09768-7
33. Verscheijden LFM, Koenderink JB, de Wildt SN, Russel FGM. Development of a physiologically-based pharmacokinetic pediatric brain model for prediction of cerebrospinal fluid drug concentrations and the influence of meningitis. *PLOS Computational Biology*. 2019;15(6):e1007117. doi:10.1371/journal.pcbi.1007117

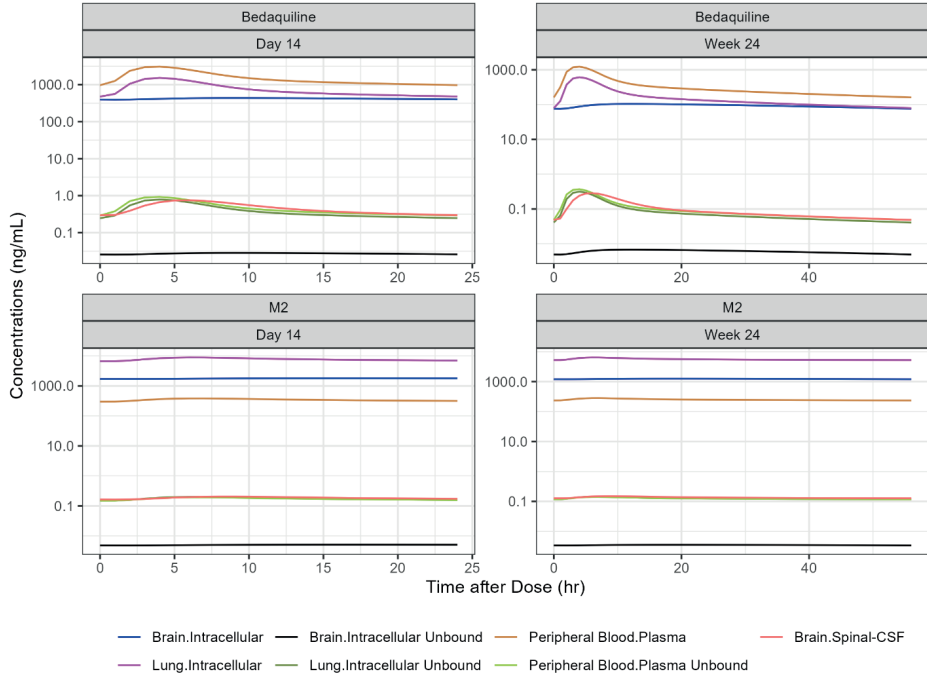
34. Utsey K, Gastonguay MS, Russell S, Freling R, Riggs MM, Elmokadem A. Quantification of the impact of partition coefficient prediction methods on physiologically based pharmacokinetic model output using a standardized tissue composition. *Drug Metabolism and Disposition*. 2020;48(10):903-916. doi:10.1124/DMD.120.090498
35. Koch S, Donarski N, Goetze K, et al. Characterization of four lipoprotein classes in human cerebrospinal fluid. *J Lipid Res*. 2001;42(7):1143-1151.
36. Conradie F, Bagdasaryan TR, Borisov S, et al. Bedaquiline–Pretomanid–Linezolid Regimens for Drug-Resistant Tuberculosis. *New England Journal of Medicine*. 2022;387(9):810-823. doi:10.1056/nejmoa2119430
37. Lippert J, Burghaus R, Edginton A, et al. Open Systems Pharmacology Community—An Open Access, Open Source, Open Science Approach to Modeling and Simulation in Pharmaceutical Sciences. *CPT: Pharmacometrics and Systems Pharmacology*. 2019;8(12):878-882. doi:10.1002/psp4.12473
38. Lounis N, Vranckx L, Gevers T, Kaniga K, Andries K. In vitro culture conditions affecting minimal inhibitory concentration of bedaquiline against *M. tuberculosis*. *Med Mal Infect*. 2016;46(4):220-225. doi:10.1016/j.medmal.2016.04.007
39. Perrineau S, Lachâtre M, Lê MP, Rioux C, Loubet P, Fréchet-Jachym M, Gonzales MC, Grall N, Bouvet E, Veziris N, Yazdanpanah Y, Peytavin G. Long-term plasma pharmacokinetics of bedaquiline for multidrug- and extensively drug-resistant tuberculosis. *Int J Tuberc Lung Dis*. 2019 Jan 1;23(1):99-104. doi: 10.5588/ijtld.18.0042.
40. Ngwalero P, Brust JCM, van Beek SW, Wasserman S, Maartens G, Meintjes G, Joubert A, Norman J, Castel S, Gandhi NR, Denti P, McIlleron H, Svensson EM, Wiesner L. Relationship between Plasma and Intracellular Concentrations of Bedaquiline and Its M2 Metabolite in South African Patients with Rifampin-Resistant Tuberculosis. *Antimicrob Agents Chemother*. 2021 Oct 18;65(11):e0239920. doi: 10.1128/AAC.02399-20.
41. Svensson EM, Dian S, Te Brake L, Ganiem AR, Yunivita V, van Laarhoven A, Van Crevel R, Ruslami R, Aarnoutse RE. Model-Based Meta-analysis of Rifampicin Exposure and Mortality in Indonesian Tuberculous Meningitis Trials. *Clin Infect Dis*. 2020 Nov 5;71(8):1817-1823. doi: 10.1093/cid/ciz1071.
42. Van Essen DC, Donahue CJ, Glasser MF. Development and Evolution of Cerebral and Cerebellar Cortex. *Brain Behav Evol*. 2018;91(3):158-169. doi: 10.1159/000489943.
43. Ruslami R, Ganiem AR, Dian S, Apriani L, Achmad TH, van der Ven AJ, Borm G, Aarnoutse RE, van Crevel R. Intensified regimen containing rifampicin and moxifloxacin for tuberculous meningitis: an open-label, randomised controlled phase 2 trial. *Lancet Infect Dis*. 2013 Jan;13(1):27-35. doi: 10.1016/S1473-3099(12)70264-5.
44. Maranchick NF, Alshaer MH, Smith AGC, Avaliani T, Gujabidze M, Bakuradze T, Sabanadze S, Avaliani Z, Kipiani M, Peloquin CA, Kempker RR. Cerebrospinal fluid concentrations of fluoroquinolones and carbapenems in tuberculosis meningitis. *Front Pharmacol*. 2022 Dec 12;13:1048653. doi: 10.3389/fphar.2022.1048653.

Supplementary Materials

S6.1. Summary of the Time Course Data Used for the Analysis.

Details	Source
Model Development	
Bedaquiline and M2 concentrations from blood serum of pulmonary TB patients after bedaquiline dosing of 400 mg on Day1, 300 mg on Day2, and 200 mg QD Day 3-14	Clinical Trial: NCT 01691534
Model Validation	
Bedaquiline concentrations from blood serum of pulmonary TB patients after bedaquiline dosing of 200 mg on Day1, 100 mg QD Day 2-14	Clinical Trial: NCT01215110
Bedaquiline concentrations from blood serum of pulmonary TB patients after bedaquiline dosing of 400 mg on Day1, 300 mg on Day2, and 200 mg QD Day 3-14	
Bedaquiline concentrations from blood serum of pulmonary TB patients after bedaquiline dosing of 500 mg on Day1, 400 mg on Day2, and 300 mg QD Day 3-14	
Bedaquiline concentrations from blood serum of pulmonary TB patients after bedaquiline dosing of 700 mg on Day1, 500 mg on Day2, and 400 mg QD Day 3-14	
Steady-state concentrations of bedaquiline and M2 from blood serum and CSF of pulmonary TB patients following bedaquiline dosing of 400 mg QD for 14 days followed by 200 mg three times a week	Clinical Trial: NCT02583048

S6.2. Typical Patient Simulations of Bedaquiline and M2 Concentrations within Various Compartments Following the Current Bedaquiline Dosing Regimens. The simulations suggested limited availability of unbound bedaquiline and M2 in brain intracellular compartment. Dosing regimen, 400 mg QD for 14 days followed by 200 mg three times a week was simulated.



S6.3. Final model files are available to download from https://github.com/krinaj/BDQ_PBPk.

